IOP Conf. Series: Materials Science and Engineering **269** (2017) 012081 doi:10.1088/1757-899X/269/1/012081

Structure and Mechanical Properties of the AlSi10Mg Alloy Samples Manufactured by Selective Laser Melting

Xiaodan Li[1], Jiaqiang Ni[1], Qingfeng Zhu[2], Hang Su[1], Jianzhong Cui[2], Yifei Zhang[3], Jianzhong Li[3*]

[1]Shenyang aircraft industry (Group) Co., Ltd., Shenyang, 110819, China
[2]Key Laboratory of Electromagnetic Processing of Materials, Ministry of Education Northeastern University, Shenyang, 110819, China
[3]School of Metallurgy, Northeastern University, Shenyang, 110819, China

Abstract. The AlSi10Mg alloy samples with the size of 14×14×91mm were produced by the selective laser melting (SLM) method in different building direction. The structures and the properties at -70°C of the sample in different direction were investigated. The results show that the structure in different building direction shows different morphology. The fish scale structures distribute on the side along the building direction, and the oval structures distribute on the side vertical to the building direction. Some pores in with the maximum size of 100 μm exist of the structure. And there is no major influence for the build orientation on the tensile properties. The tensile strength and the elongation of the sample in the building direction are 340 Mpa and 11.2 % respectively. And the tensile strength and the elongation of the sample vertical to building direction are 350 Mpa and 13.4 % respectively

1. Introduction

As one kind of additive manufacturing method, selective laser melting (SLM) is now widely used for various materials [1-11]. Recently, the SLM power-bed technology has been widely concerned by aerospace manufacturers for it can realize the “rapid manufacturing” of complicated metallic components [1, 10, 11]. There have been an increasing number of reports on SLM of Al-alloys recently, because of the demand from the aircraft industry for lightweight structures with complex geometries [9, 11]. Among the various aluminum alloys, the AlSi10Mg seem better suited to the SLM technology for the good mechanical properties and process performance. And various reports have been published to study the structure and properties of SLM-preparation AlSi10Mg [8, 11-13].

This paper focuses on the mechanical properties of the selective laser melting AlSi10Mg alloy at low temperature. The influence of the building direction (vertical and horizontally built samples) on the tensile properties at -70°C was investigated. In addition, the fracture morphology and the structure near the facture also were investigated.

2. Experimental procedures

The chemical composition of the AlSI10Mg power is shown in table 1. Figure 1 shows a SEM (scanning electron microscope) micrograph of the power. It is shown that the particles of the power are not all spherical. Many irregular morphology particles with different size distribute in the power. The size range of the particles was 15-70 μm, and the average size of the particles is about 40 μm.

Table 1. Chemical composition of the investigated AlSI10Mg alloy (wt. %).

Al	Si	Fe	Cu	Mn	Mg	Zn	Cr	Ni	Ti
89.6	9.80	0.158	0.005	0.004	0.363	0.0015	0.007	0.005	0.004

The specimens with the size of 14×14×91 mm (as shown in figure 2) were preparation by a SLM (laser powder-bed) system. And the argon was employed to protect the whole building processing. In order to get the specimens in different building direction, the specimens were built along Z and Y direction respectively, as shown in figure 2. This means that the long boundary of the sample is perpendicular and parallel to the building direction respectively. The specimen was cut in the transverse direction (X-Z plane in figure 2). And then, the specimen was polished and etched for metallurgical analysis.

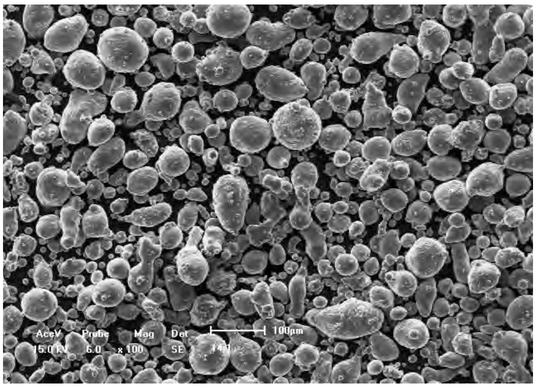

Figure 1. Morphology of the AlSi10Mg power under SEM.

Figure 2. The specimen fabricated by the SLM.

3. Mechanical testing

The specimens in different building direction were machined to standard tensile samples. The tensile test geometry is shown in figure 3. Tensile tests were conducted on a Sans type tensile testing machine with the tensile speed of the 1 mm/min at -70°C. And all the mechanical test results are the average of 3 samples. The fracture surface was analyzed by a Shimadzu SSX-550 scanning electron microscope. And the microstructure near the fracture was investigated by the optical microscope.

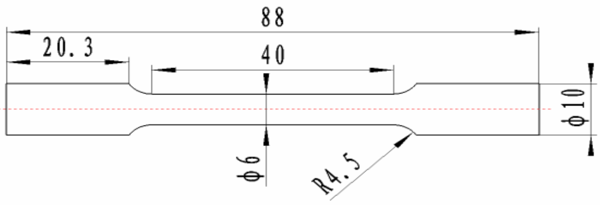

Figure 3. Tensile test samples and sample geometry.

4. Results and discussion

Figure 4 shows the three dimensional macrostructure of the specimen. B is surface formed after the last laser scanning. It is shown that the traces of laser scanning parallel distribute along the scanning direction on surface B. C is the original side surface built during laser scanning layer by layer. This surface is pretty rough, and many of cavities and unmelted AlSi10Mg particles exist on surface C. Surface A is the transverse section (which cut along the building direction) of the specimen. The inner structure of the specimen is revealed in this section. It is shown that the "fish scale" structure distribute on this section.

Figure 5 shows the microstructure of the specimen in different transverse section. It is shown that the microstructure in different transverse section is difference. The oval structures along different direction distribute on the section parallel to the scanning surface, and many black pores with the size less than 50 μm exist in this section as shown in figure 5 (a). While, the fish scale structure distribute on the section vertical to the scanning surface, and many black pores (with the size about 100 μm) exist in this section as shown in figure 5 (b). Oval structures along different direction show the top view of the melt pool and suggest the scanning direction of each laser scanning layer is difference. The arc edge of the fish scale is actually consisted by the bottom of the melt pool of each laser scanning. The porosities and pores are easily formed on the edge of the fish scale during remelting and solidification process.

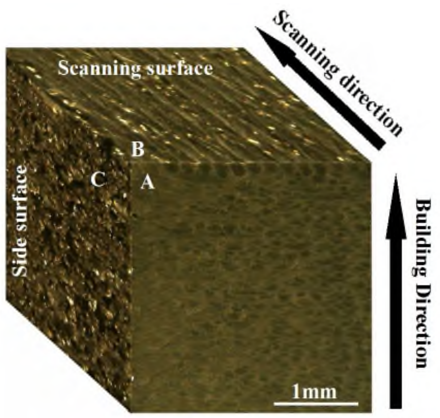

Figure 4. Optical micrographs from three orthogonal planes showing the macrostructures of the specimen.

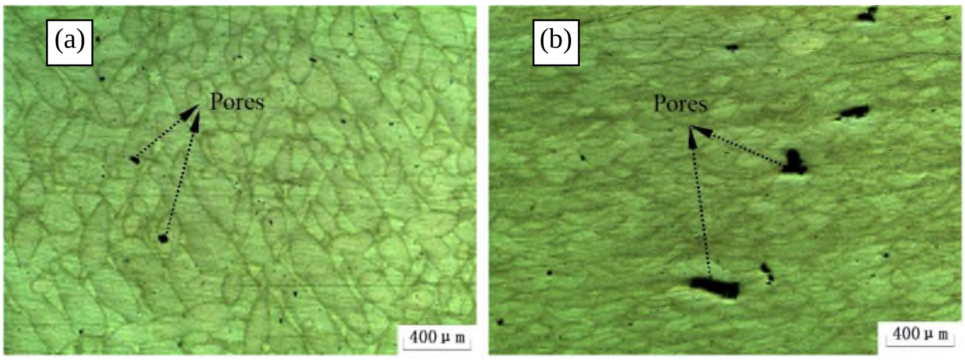

(a) parallel to surface B in figure 4, (b) the transverse section parallel to surface A in figure 4.

Figure 5. Microstructure in different t transverse section of the specimen.

The tensile strength and the elongation parallel to the building direction of the sample are 350 MPa and 11 %, respectively. The tensile strength and elongation vertical to the building direction of the sample are 340 MPa and 13 %, respectively. This indicates that the building direction has little influence on the properties of the SML specimens at low temperature.

Figure 6 shows the fracture morphology of the specimen. It is shown that the fracture morphology corresponding to different direction are quite difference. The fracture surface of the specimen pulled along the building direction displays a step like morphology, as shown in figure 6 (a). The average step size is about 100 μm, which corresponds to the size of the laser tracks. At high magnifications, the fracture surface appears to contain a mix of small dimples and smooth areas, as shown in figure 6 (b) and (c). These dimples in Al matrix are related to the pulling out the brittle Si particles. The smooth areas may be related with the pores in the specimen. The fracture surface of the specimen pulled vertical the building direction is rather irregular, as shown in figure 6 (d), and many cavities distribute on the surface of this fracture. At high magnifications, the fracture surface appears to contain a mix of small dimples and deep cavities, as shown in figure 6 (e) and (f). Moreover, there are no un-melted powders particles are observed on the surface.

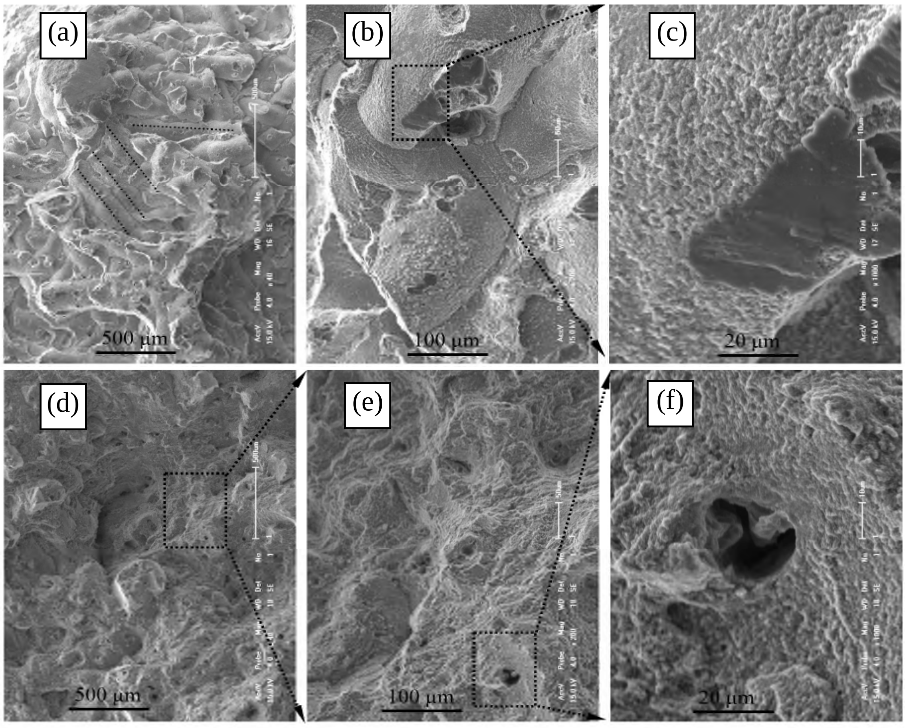

Figure 6. Fracture morphology of the specimen pulled along different direction (a) the typical fracture morphology of the specimen pulled parallel to the building direction, (b) partial enlargement of the (a), (c) partial enlargement of the (b), (d) the typical fracture morphology of the specimen pulled vertical to the building direction, (e) partial enlargement of the (d), (f) partial enlargement of the (e).

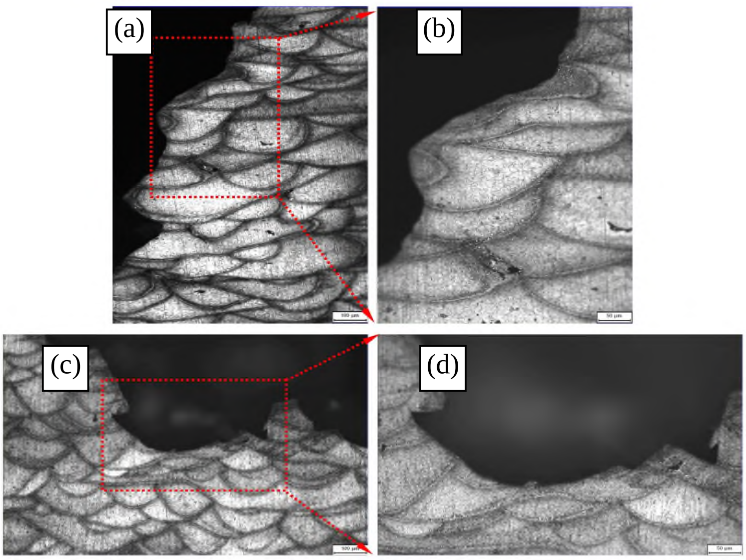

Figure 7. Microstructure near the fracture of the tensile samples. (a) microstructure of the specimen pulled vertical to the building direction, (b) partial enlargement of (a) (c) microstructure of the specimen pulled parallel to the building direction, (d) partial enlargement of (c).

Figure 7 (a) and (c) show the microstructure near the fracture of the tensile samples pulled vertical and parallel the building direction, respectively. It is can be seen that the cracks grow along the boundaries of the "fish scale" structure in two pulling direction. This suggests that the boundaries of the "fish sale" structure act as preferential sites for failure. These boundaries of the "fish sale" structure actually are the bonding zones formed during laser scanning layer by layer. In fact, many of curved surfaces consisted by the bonding zones exist in the SLM specimens and parallel to the scanning direction. When pulling along the building direction, the sample fractures along the curved surface and forms a step like morphology as shown in figure 6 (a). When the pulling direction is vertical to the building direction, the bonding zones fracture vertical to the curved surface and form rather irregular fracture morphology, as shown in figure 6.

5. Conclusion

(1) The structure in different building direction shows different morphology. The fish scale structures distribute on the side along the building direction, and the oval structures distribute on the side vertical to the building direction. Some pores in with the maximum size of 100 μm exist of the structure.

(2) There is no major influence for the build orientation on the tensile properties. The tensile strength and the elongation of the sample in the building direction are 340 Mpa and 11.2 % respectively. And the tensile strength and the elongation of the sample vertical to building direction are 350 Mpa and 13.4 % respectively.

6. Reference

[1] Amato K N, Gaytan S M, Murr L E, et al. 2012 *Acta Mater.* **60** 2229-39.
[2] Kruth J P, Froyen L, Van Vaerenbergh J, et al. 2004 *J. Mater. Process. Tech.* **149** 616-22.
[3] Thijs L, Verhaeghe F, Craeghs T, et al. 2010 *Acta Mater.* **58** 3303-12.
[4] Rombouts M, Kruth J P, Froyen L, et al. 2006 *CIRP Ann-Manuf. Techn.* **55** 187-92.
[5] Abe F, Osakada K, Shiomi M, et al. 2001 *J. Mater. Proc. Tech.* **111** 210-3.
[6] Vandenbroucke B and Kruth J P 2007 *Rapid. Prototyp. J.* **13(4)** 196-203.
[7] Louvis E, Fox P and Sutcliffe C J 2011 *J. Mater. Proc. Tech.* **211** 275-84.
[8] Brandl E, Heckenberger U, Holzinger V, et al. 2012 *Mater. Des.* **34** 159-69.
[9] Dadbakhsh S and Hao L 2012 *J. Alloy. Comp.* **541** 328-34.
[10] Gu D, Wang Z, Shen Y, et al. 2009 *Appl. Surf. Sci.* **255** 9230-40.
[11] Read N, Wang W, Essa K, et al. 2015 *Mater. Des.* **65** 417-24.
[12] Thijs L, Kempen K, Kruth J P, et al. 2013 *Acta Mater.* **61** 1809-19.
[13] Kempen K, Thijs L, Van Humbeeck J, et al. 2012 *Phys. Proc.* **339** 439-46.

Acknowledgement

The Project Supported by National Natural Science Foundation of China (No. 51204053), Central University Basic R & D Operating Expenses (No. N130409005).